University of
Strathclyde
Glasgow

This version is available at https://strathprints.strath.ac.uk/53455/

Equations for the estimation of strong ground motions from shallow crustal earthquakes using data from Europe and the Middle East: Vertical peak ground acceleration and spectral acceleration

N. N. Ambraseys, J. Douglas[*] S. K. Sarma

Department of Civil and Environmental Engineering,

Imperial College London,

South Kensington Campus,

London,

SW7 2AZ,

United Kingdom.

Tel: +44 (0)20 75946059

Fax: +44 (0)20 72252716

Email: n.ambraseys@imperial.ac.uk

and

P. M. Smit currently at:

National Emergency Operations Centre,

CH-8044 Zürich,

Switzerland.

September 13, 2004

Running title: Equations for estimation of vertical ground motions

Keywords: Strong ground motion estimation, attenuation relations, Europe, Middle East

Article type: General paper

[*]Now at: ARN/RIS; BRGM; 3 avenue C. Guillemin; BP 6009; 45060 Orléans Cedex 2; France.

Abstract

This article presents equations for the estimation of vertical strong ground motions caused by shallow crustal earthquakes with magnitudes $M_w \geq 5$ and distance to the surface projection of the fault less than $100\,\mathrm{km}$. These equations were derived by weighted regression analysis, used to remove observed magnitude-dependent variance, on a set of 595 strong-motion records recorded in Europe and the Middle East. Coefficients are included to model the effect of local site effects and faulting mechanism on the observed ground motions. The equations include coefficients to model the observed magnitude-dependent decay rate. The main findings of this study are that: short-period ground motions from small and moderate magnitude earthquakes decay faster than the commonly assumed $1/r$, the average effect of differing faulting mechanisms is similar to that observed for horizontal motions and is not large and corresponds to factors between 0.7 (normal and odd) and 1.4 (thrust) with respect to strike-slip motions and that the average long-period amplification caused by soft soil deposits is about 2.1 over those on rock sites.

1   Introduction

This is a companion article to Ambraseys *et al.* (2004) (here called Paper 1) to provide ground motion estimation equations for vertical peak ground acceleration and spectral acceleration for 5% damping. It uses the same set of data, functional form and regression method as used in Paper 1 and therefore the equations derived here for vertical motions are consistent with those derived for horizontal motions. Only a brief description of the data, functional form and regression method are given here so please see Paper 1 for more details.

Briefly, a set of 595 records were selected using a reasonably strict selection criteria that sought to limit the number of conversions and assumptions required to yield a uniform set of data. The records chosen all are from shallow ($h \leq 30\,\mathrm{km}$) crustal earthquakes in Europe and the Middle East (mainly from Italy, Greece, Turkey and Iceland) and are reasonably well distributed in terms of moment magnitude (M_w) (Kanamori, 1977) and distance to the surface projection of rupture (d_f) (Joyner and Boore, 1981), which are the magnitude scale and distance metric adopted, within the range $5.0 \leq M_w \leq 7.6$ and $0 \leq d_f \leq 100\,\mathrm{km}$. Recording sites are divided into four classes following Boore *et al.* (1993), namely: very soft soil (L) $V_{s,30} \leq 180\,\mathrm{ms}^{-1}$ (11 records), soft soil (S) $180 < V_{s,30} \leq 360\,\mathrm{ms}^{-1}$ (143 records), stiff soil (A) $360 < V_{s,30} \leq 750\,\mathrm{ms}^{-1}$ (238 records) and rock (R) $V_{s,30} > 750\,\mathrm{ms}^{-1}$ (203 records). Records from very soft soil sites were combined with those from soft soil sites because there are too few records from very soft soil sites to yield a robust site coefficient. Earthquakes were classified by style-of-faulting using the criteria of Frohlich and Apperson (1992) based on the plunges of the eigenvectors

of the moment tensor. The distribution of records with respect to faulting mechanism is: normal (191 records), strike-slip (160 records), thrust (91 records) and odd (153 records). All records were corrected using the BAP procedure (Converse and Brady, 1992) with low cut-off frequencies chosen through an examination of signal-to-noise ratio and/or by examining the Fourier amplitude spectrum and the filtered velocity and displacement traces.

In order to model the observed effect of magnitude-dependent decay rate the adopted functional form is:

$$\log y = a_1 + a_2 M_w + (a_3 + a_4 M_w) \log \sqrt{d^2 + a_5^2} + a_6 S_S + a_7 S_A + a_8 F_N + a_9 F_T + a_{10} F_O \quad (1)$$

where $S_S = 1$ for soft soil sites and 0 otherwise, $S_A = 1$ for stiff soil sites and 0 otherwise, $F_N = 1$ for normal faulting earthquakes and 0 otherwise, $F_T = 1$ for thrust faulting earthquakes and 0 otherwise and $F_O = 1$ for odd faulting earthquakes and 0 otherwise.

Weighted one-stage maximum-likelihood regression (Joyner and Boore, 1993) was used to derive the coefficients of the ground motion estimation equations. Details of how the magnitude-dependent weighting functions were calculated are given below.

2 Pure error analysis

As for horizontal motions, pure error analysis (Draper and Smith, 1981, pp. 33–42) was performed here in order to verify that the commonly used logarithmic transformation is justified; to investigate the magnitude-dependence of the scatter; and to assess the lower limit on the equations' standard deviations using only magnitude and distance. Exactly the same procedure was used here as was used in Paper 1.

2.1 Logarithmic transformation

As was done in Paper 1, the dataspace was divided into intervals of 0.2 magnitude units by $2\,\mathrm{km}$ within which the mean, η, and unbiased standard deviation, σ, of the untransformed ground motion (PGA and SA) was calculated using the maximum-likelihood method (Spudich $et\ al.$, 1999, p. 1170). Then the coefficient of variation, $V = 100\sigma/\eta$, was plotted against η for PGA and each period of SA. If σ was proportional to η then these graphs should show no trend with increasing ground motion. A linear equation $V = \alpha + \beta\eta$ was fitted to each of these graphs. The 95% confidence intervals of α and β were computed along with the standard deviation of the equation as were the computed and critical t value for $\beta = 0$ for the 5% significance level. Like for horizontal motions (Paper 1), it was found that β is not significantly different than zero for almost all of the periods investigated because computed t is not

3

bigger than critical t. Thus the null hypothesis that the scatter associated with measured ground motion is proportional to the amplitude of the ground motion cannot be rejected, so the logarithmic transformation is justified. For PGA and for SA at six periods (0.050–0.075 s) β was found to be significantly different than zero therefore suggesting that the logarithmic transformation is not justified for those periods. Interestingly the slope β is positive, suggesting that the scatter increases with increasing ground motion amplitude, which has never been suggested before. Therefore, like for horizontal motions, it was decided to apply the logarithmic transformation for the entire period range.

2.2 Dependence of scatter on magnitude

Like for horizontal motions, the derived standard deviations of each bin were plotted against M_w and best-fit lines derived. The slopes of these lines were then tested to see if they were significant at the 5% level. It was found that for certain periods (0.15–0.40 s, 0.60–0.65 s, 0.75 s and 0.85 s) the slopes of the derived lines were significantly different than zero. Consequently, these derived functions were used as weighting functions for the regression analysis, as was done in Paper 1.

The magnitude-dependency of scatter in vertical ground motions is less pronounced than it is for horizontal motions (as shown by the scatter for fewer periods displaying a significant slope than for horizontal motions). This suggests that different physical processes may be controlling the magnitude-dependence of the scatter for horizontal and vertical motions. For example, the effect of nonlinear soil behaviour in limiting ground motion amplitudes, which has been suggested as one possible cause of magnitude-dependent uncertainty (Youngs *et al.*, 1995), may be to be less important for vertical motions than for horizontal motions (e.g. Bommer *et al.*, 2004).

2.3 Lower limit on standard deviations possible using only magnitude and distance

Pure error analysis was also used to assess the lowest standard deviations possible for the derived equations. They were found to be in the range 0.21 to 0.28. Lower standard deviations than these should not be expected.

3 Results

Equations were derived for the estimation of peak ground acceleration and spectral acceleration for 5% critical damping ratio and for 61 periods between 0.05 s (20 Hz) and 2.5 s (0.4 Hz) using the Caltech spacing (Brady *et al.*, 1973). The coefficients, associated standard deviations and the number of records, earthquakes and stations used to derive each equation are reported in Table 1. The non-significant coefficients are highlighted in Table 1 although these coefficients should not be dropped when computing

ground motion estimates. As for horizontal motions no smoothing of the coefficients was attempted.

Figure 1 shows the decay of estimated vertical peak ground acceleration and spectral acceleration at $1\,\mathrm{s}$ natural period with distance for $M_w = 5$, 6 and 7 strike-slip earthquakes at a rock site. This figure shows the effect of the magnitude-dependent decay rate for short-period ground motions (e.g. peak ground acceleration) and magnitude-independent decay rate for long-period ground motions (e.g. spectral acceleration at $1\,\mathrm{s}$). The dependence of the decay rate on magnitude is less for vertical motions than it is for horizontal motions. For example, the magnitude-dependent decay coefficient, a_4, for horizontal PGA is 0.314 whereas for vertical PGA it is 0.206.

Figure 2 shows the estimated vertical response spectra for $M_w = 5$, 6 and 7 strike-slip earthquakes at 10 and at $100\,\mathrm{km}$ at a rock site. This figure shows the effect of the magnitude-dependent decay rate because at near-source distances the effect of magnitude on the spectral accelerations is less than at large source-to-site distances.

3.1 Effect of faulting mechanism

Figure 3 shows a comparison of the ratio of spectral accelerations from thrust/reverse faulting earthquakes to those from strike-slip faulting earthquakes, $F_{\mathrm{R:SS}}$, derived in this study to those in the literature. Unlike horizontal PGA and SA, there are few estimates of $F_{\mathrm{R:SS}}$ in the literature. $F_{\mathrm{R:SS}}$ derived here is only significantly different than one at the 5% level for the periods $0.24\,\mathrm{s}$, 0.38–$0.40\,\mathrm{s}$ and 0.60–$1.00\,\mathrm{s}$. Figure 3 shows that the factor derived here matches closely to those derived previously and corresponds to a maximum factor of about 1.4, which is higher than the factor derived for horizontal motions, which had a maximum of about 1.3.

Figure 4 shows the derived ratios of spectral accelerations caused by normal faulting earthquakes and from earthquakes whose mechanism is defined as odd to those from strike-slip earthquakes, $F_{\mathrm{N:SS}}$ and $F_{\mathrm{O:SS}}$ respectively. $F_{\mathrm{N:SS}}$ is only significantly different than one at the 5% level for periods shorter than $0.14\,\mathrm{s}$ and for $1.60\,\mathrm{s}$ and $F_{\mathrm{O:SS}}$ is only significantly different than one at the 5% level for the period range 0.11–$0.12\,\mathrm{s}$. Figure 4 shows that there is evidence for smaller short-period ground motions from normal faulting earthquakes than strike-slip earthquakes (factor of about 0.7) but that for most periods the amplitudes of ground motions from normal and strike-slip earthquakes are similar. For long periods, ground motion amplitudes from normal faulting earthquakes are higher than those from strike-slip earthquakes. Figure 4 also shows that long-period spectral accelerations from earthquakes classified as odd are lower (factor of about 0.9) than those from strike-slip earthquakes but note that this observed difference in ground motions is not significant at almost all periods.

3.2 Effect of local site conditions

Figure 5 shows a comparison between the local site amplification factors for soft soil sites and stiff soil sites derived in this study and those derived in some previous studies. $F_{\text{softsoil:rock}}$ is significant for almost all periods and gives an average amplification over rock motions of about 2.1 at about $1.5\,\text{s}$, which is much higher than the amplifications derived by other studies. $F_{\text{stiffsoil:rock}}$ is significant for most periods longer than $0.15\,\text{s}$ and reaches a maximum amplification of about 1.5 at $1.5\,\text{s}$, which is lower than those by Campbell and Bozorgnia (2003) and higher than those by Ambraseys and Simpson (1996) and Lussou *et al.* (2001).

3.3 Comparisons to previous equations

The estimated ground motions from the equations derived in this study were compared with Ambraseys and Simpson (1996) and Campbell and Bozorgnia (2003). Ambraseys and Simpson (1996) used M_s rather than M_w, hence a conversion needs to be undertaken; this was done using the equations of Ekström and Dziewonski (1988). Campbell and Bozorgnia (2003) use seismogenic distance rather than distance to the surface projection of the fault and consequently a conversion needs to be applied. The comparison was made for a vertical strike-slip fault with a non-seismogenic layer of $3\,\text{km}$ thickness at the top of the crust.

Figure 6 shows that the estimated response spectra from the equations derived here match the estimated response spectra given by the equations of Ambraseys and Simpson (1996) for moderate and large magnitudes at all distances covered by the equations. Whereas the estimated response spectra given by the new equations for small magnitudes are above the spectra given by Ambraseys and Simpson (1996) for short distances and below for long distances. This is because the equations of Ambraseys and Simpson (1996) assumed a magnitude-independent decay rate that, due to the distribution of data (most records from long distances are from moderate and large magnitude earthquakes), corresponds to the decay rate of large earthquakes. The equations presented here predict a much faster decay rate for small earthquakes (-1.458 compared to -0.954 for PGA from a $M_w = 5$ earthquake) and consequently the estimated ground motions from small earthquakes at large distances are lower than those predicted by Ambraseys and Simpson (1996). This suggests that small earthquakes at large distances are less important than would be assumed by using the equations of Ambraseys and Simpson (1996).

Figure 7 shows that the ground motion estimates from the equations presented here match those given by the equations of Campbell and Bozorgnia (2003) for the magnitudes and distances considered here except at large distances from small earthquakes, again since Campbell and Bozorgnia (2003) had little data from such magnitudes and distances in their construction set.

4 Residuals

Table 2 gives the median amplification factor (computed by taking the anti-logarithm of the mean residuals for that station) over the median ground motion estimates for the strong-motion stations that have recorded five or more earthquakes. It shows that for some stations there is a considerable local site amplification. For example, like for horizontal motions the stations at Nocera Umbra show an amplification factor of up to 3.14 at a natural period of $0.2\,\mathrm{s}$. Another station that shows considerable amplification is Gubbio-Piana, which has a median amplification of 11.51 at a natural period of $2\,\mathrm{s}$. This station is in a sedimentary basin, which amplifies the long-period ground motions. Records from this station often show clear surface waves. One station that shows considerably lower than expected short-period spectral accelerations is Yarimca-Petkim, which also shows lower horizontal motions (see Paper 1).

Table 3 gives the median amplification factor for the ten best recorded earthquakes. It shows that most earthquakes do not show a significant deviation from the median (most factors are about one). Like for horizontal motions, there is evidence that the ground motions from the Umbria Marche sequence are higher than would be expected for such sized earthquakes. Also, as for horizontal motions, this analysis suggests that ground motions recorded during the Düzce (12/11/1999) earthquake are lower than would be expected from such an earthquake.

Figure 8 shows graphs of the normalised residuals against M_w and distance for PGA and spectral acceleration at $1\,\mathrm{s}$ natural period. All the residual plots examined show no obvious dependence of the scatter on magnitude or distance. The apparent constant bias in the residual plot for spectral acceleration at $1\,\mathrm{s}$ natural period is common to all graphs of residuals for long-period motions. It is caused by the use of the maximum-likelihood regression method since it splits the error into intra- and inter-earthquake portions.

5 Conclusion

This article presents equations for the estimation of vertical peak ground acceleration and spectral acceleration for 5% damping for periods between 0.05 and $2.5\,\mathrm{s}$. Since the equations presented here were derived using an identical set of records and method to those derived in Paper 1 for horizontal motions the equations are mutually consistent and therefore can be used to investigate the relationship between vertical and horizontal response spectra (e.g. Campbell and Bozorgnia, 2003).

The main conclusions of this article are similar to those for horizontal motions given in Paper 1. It has been found that the equations derived here predict similar spectral accelerations to commonly-used equations for moderate and large magnitudes but that the new equations predict lower ground motions

from small earthquakes at large distances. Therefore, the use of the equations presented here will reduce the importance of ground motions from small earthquakes at large distances in seismic hazard analysis. The effect of local site conditions in the new equations is greater than that found in many previous studies, e.g. the estimated average amplification at soft soil sites at long-periods is about 2.1 over that recorded at rock sites. The new equations also include factors to model the difference in ground motions between different earthquakes with different faulting mechanisms. Average intermediate-period vertical ground motions from thrust/reverse faulting earthquakes are up to 1.4 times higher than those from strike-slip earthquakes. Short-period vertical ground motions from normal faulting earthquakes are about 0.8 those from strike-slip earthquakes. As for the equations for horizontal motions the associated standard deviations are not significantly less than in previous studies, again highlighting the need to include more independent variables into empirical ground motion estimation equations.

Acknowledgements

References

Abrahamson, N. A. and J. J. Litehiser (1989). Attenuation of vertical peak acceleration. *Bulletin of the Seismological Society of America* **79**, 549–580.

Abrahamson, N. A. and W. J. Silva (1997). Empirical response spectral attenuation relations for shallow crustal earthquakes. *Seismological Research Letters* **68**, 94–127.

Ambraseys, N. N., J. Douglas, S. K. Sarma, and P. M. Smit (2004). Equations for the estimation of strong ground motions from shallow crustal earthquakes using data from Europe and the Middle East: Horizontal peak ground acceleration and spectral acceleration. *Bulletin of Earthquake Engineering* **3**. In press.

Ambraseys, N. N. and K. A. Simpson (1996). Prediction of vertical response spectra in Europe. *Earthquake Engineering and Structural Dynamics* **25**, 401–412.

Aptikaev, F. and J. Kopnichev (1980). Correlation between seismic vibration parameters and type of faulting. In *Proceedings of Seventh World Conference on Earthquake Engineering*, volume 1, 107–110.

Bommer, J. J., N. A. Abrahamson, F. O. Strasser, A. Pecker, P.-Y. Bard, H. Bungum, F. Cotton, D. Fäh, F. Sabetta, F. Scherbaum, and J. Studer (2004). The challenge of defining upper bounds on earthquake ground motions. *Seismological Research Letters* **75**, 82–95.

Boore, D. M., W. B. Joyner, and T. E. Fumal (1993). Estimation of response spectra and peak accelerations from western North American earthquakes: An interim report. Open-File Report 93-509, U.S. Geological Survey. 70 pages.

Brady, A. G., M. D. Trifunac, and D. E. Hudson (1973). Analyses of strong motion earthquake accelerograms — response spectra. Technical report, Earthquake Engineering Research Laboratory — California Institute of Technology.

Campbell, K. W. and Y. Bozorgnia (2003). Updated near-source ground-motion (attenuation) relations for the horizontal and vertical components of peak ground acceleration and acceleration response spectra. *Bulletin of the Seismological Society of America* **93**, 314–331.

Converse, A. M. and A. G. Brady (1992). BAP basic strong-motion accelerogram processing software, version 1.0. Open-File Report 92-296A, US Geological Survey.

Draper, N. R. and H. Smith (1981). *Applied Regression Analysis*. 2nd edition. John Wiley & Sons.

Ekström, G. and A. M. Dziewonski (1988). Evidence of bias in estimations of earthquake size. *Nature* **332**, 319–323.

Frohlich, C. and K. D. Apperson (1992). Earthquake focal mechanisms, moment tensors, and the consistency of seismic activity near plate boundaries. *Tectonics* **11**, 279–296.

Joyner, W. B. and D. M. Boore (1981). Peak horizontal acceleration and velocity from strong-motion records including records from the 1979 Imperial Valley, California, earthquake. *Bulletin of the Seismological Society of America* **71**, 2011–2038.

Joyner, W. B. and D. M. Boore (1993). Methods for regression analysis of strong-motion data. *Bulletin of the Seismological Society of America* **83**, 469–487.

Kanamori, H. (1977). The energy release in great earthquakes. *Journal of Geophysical Research* **82**, 2981–2987.

Lussou, P., P. Y. Bard, F. Cotton, and Y. Fukushima (2001). Seismic design regulation codes: Contribution of K-Net data to site effect evaluation. *Journal of Earthquake Engineering* **5**, 13–33.

Spudich, P., W. B. Joyner, A. G. Lindh, D. M. Boore, B. M. Margaris, and J. B. Fletcher (1999). SEA99: A revised ground motion prediction relation for use in extensional tectonic regimes. *Bulletin of the Seismological Society of America* **89**, 1156–1170.

Youngs, R. R., N. Abrahamson, F. I. Makdisi, and K. Sadigh (1995). Magnitude-dependent variance of peak ground acceleration. *Bulletin of the Seismological Society of America* **85**, 1161–1176.

Period	a_1	a_2	a_3	a_4	a_5	a_6	a_7	a_8	a_9	a_{10}	σ_1	σ_2	N_{rec}	N_{eq}	N_{st}
PGA	0.835	*0.083*	-2.489	0.206	5.6	0.078	*0.046*	-0.126	*0.005*	*-0.082*	0.262	0.100	595	135	338
0.050	1.426	*0.053*	-2.681	0.217	4.7	0.090	*0.039*	-0.168	*0.005*	*-0.070*	0.301	0.115	595	135	338
0.055	1.330	*0.077*	-2.598	0.200	5.1	0.086	*0.041*	-0.162	*-0.009*	*-0.067*	0.296	0.112	595	135	338
0.060	1.333	*0.090*	-2.601	0.195	5.7	0.091	*0.051*	-0.171	*-0.016*	*-0.069*	0.295	0.111	595	135	338
0.065	1.261	*0.106*	-2.538	0.185	6.0	0.082	*0.058*	-0.172	*-0.026*	*-0.078*	0.292	0.109	595	135	338
0.070	1.231	*0.107*	-2.497	0.183	6.1	0.081	*0.050*	-0.164	*-0.011*	*-0.083*	0.290	0.106	595	135	338
0.075	1.119	*0.119*	-2.403	0.173	6.0	0.079	*0.047*	-0.149	*-0.011*	*-0.077*	0.290	0.106	595	135	338
0.080	0.947	*0.143*	-2.287	0.158	5.8	0.075	*0.045*	-0.142	*-0.013*	*-0.075*	0.293	0.108	595	135	338
0.085	0.794	*0.169*	-2.171	0.140	6.1	0.070	*0.047*	-0.132	*0.000*	*-0.078*	0.295	0.108	595	135	338
0.090	0.721	*0.181*	-2.123	0.132	6.5	0.078	*0.054*	-0.118	*0.012*	*-0.083*	0.294	0.106	595	135	338
0.095	0.695	0.187	-2.119	0.131	6.7	0.081	*0.055*	-0.116	*0.007*	*-0.089*	0.287	0.106	595	135	338
0.100	0.844	*0.166*	-2.217	0.146	7.1	0.083	*0.050*	-0.108	*0.003*	*-0.091*	0.287	0.106	595	135	338
0.110	0.990	*0.145*	-2.270	0.154	7.8	0.079	*0.057*	-0.105	*-0.014*	-0.100	0.285	0.104	595	135	338
0.120	0.830	*0.168*	-2.133	0.136	7.9	0.065	*0.054*	-0.104	*-0.025*	*-0.091*	0.281	0.105	595	135	338
0.130	0.655	0.189	-2.048	0.127	7.7	*0.053*	*0.045*	-0.090	*-0.013*	*-0.087*	0.278	0.104	595	135	338
0.140	0.600	*0.179*	-2.012	0.132	6.7	*0.057*	*0.055*	-0.084	*-0.006*	*-0.084*	0.282	0.103	595	135	338
0.150	0.824	*0.130*	-2.107	0.152	6.4	0.077	0.058	-0.082	*0.009*	*-0.084*	0.554-$0.045M_w$	0.203-$0.017M_w$	595	135	338
0.160	0.798	*0.116*	-2.093	0.160	5.6	0.079	*0.050*	-0.067	*0.036*	*-0.078*	0.619-$0.056M_w$	0.220-$0.020M_w$	595	135	338
0.170	0.989	*0.087*	-2.262	0.185	6.0	0.089	*0.045*	-0.054	*0.051*	*-0.080*	0.684-$0.067M_w$	0.242-$0.024M_w$	595	135	338
0.180	0.764	*0.119*	-2.160	0.170	5.9	0.099	0.056	*-0.045*	*0.053*	*-0.077*	0.607-$0.055M_w$	0.216-$0.020M_w$	595	135	338
0.190	0.798	*0.112*	-2.208	0.177	6.3	0.107	0.057	*-0.035*	*0.059*	*-0.074*	0.591-$0.053M_w$	0.204-$0.018M_w$	595	135	338
0.200	0.758	*0.113*	-2.182	0.174	6.3	0.111	0.056	*-0.025*	*0.073*	*-0.068*	0.625-$0.059M_w$	0.212-$0.020M_w$	595	135	338
0.220	0.907	*0.082*	-2.319	0.197	5.9	0.117	0.072	*-0.029*	*0.088*	*-0.051*	0.672-$0.067M_w$	0.235-$0.023M_w$	595	135	338
0.240	1.165	*0.038*	-2.543	0.231	6.7	0.118	0.091	*-0.039*	0.094	*-0.056*	0.613-$0.057M_w$	0.213-$0.020M_w$	595	135	338
0.260	1.238	*0.016*	-2.590	0.245	6.2	0.111	0.082	*-0.051*	0.078	*-0.071*	0.670-$0.067M_w$	0.238-$0.024M_w$	595	135	338
0.280	1.165	*0.020*	-2.594	0.249	5.9	0.112	0.083	*-0.042*	0.066	*-0.064*	0.605-$0.056M_w$	0.217-$0.020M_w$	595	135	338
0.300	0.986	*0.053*	-2.574	0.242	6.1	0.111	0.082	*-0.047*	0.070	*-0.052*	0.569-$0.051M_w$	0.215-$0.019M_w$	595	135	338
0.320	0.685	*0.104*	-2.402	0.212	6.4	0.103	0.070	*-0.055*	0.068	*-0.056*	0.572-$0.051M_w$	0.216-$0.019M_w$	595	135	338
0.340	0.398	*0.144*	-2.251	0.189	6.4	0.110	0.071	*-0.042*	0.071	*-0.056*	0.537-$0.047M_w$	0.205-$0.018M_w$	595	135	338
0.360	0.333	0.146	-2.247	0.191	6.3	0.120	0.072	*-0.031*	0.082	*-0.055*	0.544-$0.048M_w$	0.209-$0.019M_w$	595	135	338
0.380	0.579	*0.097*	-2.415	0.221	6.2	0.128	0.077	*-0.023*	0.098	*-0.061*	0.577-$0.054M_w$	0.224-$0.021M_w$	595	135	338
0.400	0.704	*0.075*	-2.502	0.234	6.2	0.127	0.087	*-0.025*	0.108	*-0.069*	0.551-$0.049M_w$	0.215-$0.019M_w$	594	134	338
0.420	0.318	*0.135*	-2.345	0.209	6.1	0.129	0.103	*-0.034*	0.090	*-0.078*	0.270	0.103	594	134	338
0.440	0.446	*0.110*	-2.466	0.230	6.5	0.130	0.101	*-0.017*	0.081	*-0.081*	0.272	0.101	594	134	338
0.460	0.391	*0.113*	-2.478	0.233	6.8	0.136	0.103	*0.002*	0.082	*-0.070*	0.272	0.102	594	134	338
0.480	0.253	*0.132*	-2.455	0.228	6.8	0.147	0.105	*0.017*	0.085	*-0.052*	0.273	0.105	594	134	338
0.500	0.075	*0.154*	-2.381	0.219	6.6	0.151	0.103	*0.026*	0.092	*-0.047*	0.275	0.108	592	134	338
0.550	-0.147	0.178	-2.334	0.216	6.5	0.149	0.108	*0.027*	0.099	*-0.029*	0.273	0.115	591	134	338
0.600	0.193	*0.095*	-2.521	0.258	5.5	0.167	0.099	*0.037*	0.125	*-0.037*	0.602-$0.056M_w$	0.259-$0.024M_w$	589	134	336
0.650	-0.036	*0.131*	-2.463	0.244	6.0	0.187	0.107	*0.047*	0.125	*-0.024*	0.569-$0.050M_w$	0.239-$0.021M_w$	587	134	335
0.700	-0.508	0.217	-2.337	0.216	6.7	0.208	0.114	*0.033*	0.113	*-0.013*	0.284	0.120	578	132	332
0.750	-0.429	0.187	-2.326	0.220	6.0	0.219	0.109	*0.044*	0.157	*-0.026*	0.587-$0.052M_w$	0.245-$0.022M_w$	568	132	328
0.800	-0.617	0.214	-2.339	0.223	6.4	0.251	0.140	*0.018*	0.130	*-0.060*	0.278	0.118	548	128	323
0.850	-0.272	*0.143*	-2.512	0.255	6.0	0.261	0.120	*0.051*	0.163	*-0.056*	0.598-$0.055M_w$	0.248-$0.023M_w$	544	127	320
0.900	-0.786	0.220	-2.377	0.236	5.6	0.281	0.138	*0.028*	0.142	*-0.074*	0.277	0.121	531	125	313
0.950	-1.112	0.272	-2.208	0.208	5.7	0.281	0.126	*0.032*	0.144	*-0.081*	0.277	0.119	512	122	304
1.000	-1.200	0.296	-2.185	0.196	6.7	0.269	0.117	*0.050*	0.145	*-0.073*	0.278	0.115	490	116	295
1.100	-1.594	0.361	-2.017	0.164	7.3	0.269	0.117	*0.049*	*0.113*	*-0.070*	0.286	0.113	475	112	290
1.200	-1.754	0.383	-2.033	0.163	7.8	0.284	0.141	*0.053*	*0.104*	*-0.055*	0.279	0.118	459	107	284
1.300	-1.838	0.391	-2.059	0.167	8.0	0.302	0.151	*0.049*	*0.077*	*-0.062*	0.282	0.121	442	102	275
1.400	-2.296	0.457	-1.787	*0.123*	8.9	0.313	0.174	*0.100*	*0.067*	*-0.052*	0.279	0.110	408	96	263
1.500	-2.616	0.507	-1.581	*0.088*	9.3	0.319	0.178	*0.102*	*0.054*	*-0.078*	0.285	0.108	379	90	246

continued on next page

Period	a_1	a_2	a_3	a_4	a_5	a_6	a_7	a_8	a_9	a_{10}	σ_1	σ_2	N_{rec}	N_{eq}	N_{st}
1.600	-2.596	0.526	-1.692	*0.089*	11.9	0.313	0.184	0.124	*0.049*	*-0.067*	0.291	0.111	358	87	239
1.700	-2.512	0.518	-1.835	*0.106*	12.8	0.305	0.176	*0.104*	*0.036*	*-0.080*	0.296	0.117	358	87	239
1.800	-2.947	0.550	-1.661	*0.099*	9.1	0.313	0.154	*0.076*	*0.053*	*-0.110*	0.292	0.129	319	81	217
1.900	-3.007	0.556	-1.640	*0.095*	8.7	0.307	0.146	*0.060*	*0.047*	*-0.128*	0.294	0.129	319	81	217
2.000	-2.711	0.531	-1.655	*0.083*	11.8	0.319	0.171	*0.051*	*0.113*	*-0.148*	0.290	0.126	260	72	185
2.100	-2.765	0.531	-1.663	*0.085*	11.7	0.318	0.170	*0.056*	*0.128*	*-0.155*	0.291	0.128	260	72	185
2.200	-2.677	0.502	-1.781	*0.111*	11.1	0.306	0.145	*0.058*	*0.140*	*-0.156*	0.293	0.132	260	72	185
2.300	-3.340	0.616	-1.287	*0.031*	11.1	0.234	*0.112*	*0.024*	*0.122*	*-0.111*	0.297	0.131	208	59	146
2.400	-3.490	0.623	-1.265	*0.035*	10.2	0.228	*0.112*	*0.018*	*0.114*	*-0.110*	0.291	0.131	208	59	146
2.500	-3.731	0.633	-1.182	*0.035*	7.7	0.221	*0.097*	*0.012*	*0.092*	*-0.098*	0.283	0.135	207	59	145

Table 2: Average bias for the stations that have recorded five or more earthquakes.

Name	Site class	PGA	0.1 s	0.2 s	0.5 s	1.0 s	2.0 s
Assisi-Stallone	R	1.52	1.72	2.20	1.82	1.36	—
Bevagna	A	1.41	1.62	2.12	3.72	—	—
Colfiorito	A	1.13	1.09	1.59	3.30	—	—
Düzce-Meteoroloji Mudurlugu	S	1.06	1.07	0.98	0.50	—	—
Forgaria-Cornio	A	1.27	1.12	2.47	1.53	—	—
Gubbio-Piana	S	1.69	1.95	3.00	3.63	6.33	11.51
Hella	A	0.61	0.70	0.56	0.54	—	—
Kobarid-Osn.Skola	A	1.70	1.98	2.28	—	—	
Kyparrisia-Agriculture Bank	R	0.83	0.68	1.42	0.92	—	—
Lefkada-OTE Building	S	1.57	1.47	1.75	1.82	—	—
Nocera Umbra	R	2.22	2.06	3.14	2.24	2.34	—
Nocera Umbra 2	R	2.06	1.83	2.38	1.08	0.93	—
Nocera Umbra-Biscontini	R	1.25	1.07	1.01	0.89	—	—
Rieti	L	0.80	0.79	1.34	1.36	2.31	1.22
Yarimca-Petkim	S	0.65	0.53	0.83	1.00	1.53	—
Zakynthos-OTE Building	A	1.16	1.12	1.81	1.94	—	—

Table 3: Average bias for the ten best recorded earthquakes (13 records or more).

Name	M_w	Mech.	PGA	0.1 s	0.2 s	0.5 s	1.0 s	2.0 s
Campano Lucano (23/11/1980)	6.9	N	0.87	0.94	1.18	1.55	2.01	—
Umbria Marche (26/9/1997 09:40)	6.0	N	1.24	1.29	1.75	2.15	—	—
Umbria Marche (6/10/1997)	5.5	N	1.65	1.67	2.43	2.58	—	—
Umbria Marche (3/4/1998)	5.1	N	1.56	1.69	1.67	1.94	—	—
Kocaeli (17/8/1999)	7.6	S	0.80	0.82	0.94	0.81	0.78	0.66
Kocaeli aftershock (13/9/1999)	5.8	O	1.13	0.98	1.16	1.71	1.70	2.31
Kocaeli (31/8/1999)	5.1	O	0.82	0.81	0.80	1.32	1.56	—
Düzce (12/11/1999)	7.2	O	0.46	0.43	0.58	0.49	0.62	—
South Iceland (17/6/2000)	6.5	S	1.06	1.03	0.92	0.89	1.02	1.32
South Iceland (21/6/2000)	6.4	S	0.62	0.62	0.70	0.76	0.97	1.78

Figure captions

1. Decay of vertical peak ground acceleration and spectral acceleration at $1\,\mathrm{s}$ natural period from magnitude $M_w = 5$, 6 and 7 strike-slip earthquakes at rock sites.

   a. PGA.

   b. SA at $1\,\mathrm{s}$ natural period.

2. Estimated vertical spectral acceleration for $M_w = 5$, 6 and 7 strike-slip earthquakes at 10 and $100\,\mathrm{km}$ at a rock site.

   a. $10\,\mathrm{km}$.

   b. $100\,\mathrm{km}$.

3. Comparison of the ratio of vertical spectral accelerations from thrust faulting earthquakes to those from strike-slip faulting earthquakes derived in this study to those in the literature.

4. Ratios of vertical spectral accelerations from normal faulting earthquakes and earthquakes whose mechanism is defined as odd to those from strike-slip faulting earthquakes.

5. Comparison of estimated ratio of vertical peak ground acceleration and response spectral amplitudes for ground motions on: a) soft soil sites and hard rock sites and on: b) stiff soil sites and hard rock sites, for three recent equations to estimate strong ground motions. Soft soil sites were assumed to have an average shear-wave velocity in the top $30\,\mathrm{m}$ of $310\,\mathrm{ms}^{-1}$ and hence be within category S ($180 < V_{s,30} \le 360\,\mathrm{ms}^{-1}$) of Ambraseys and Simpson (1996) and category C ($200 < V_{s,30} \le 400\,\mathrm{ms}^{-1}$) of Lussou *et al.* (2001) and for the equations of Campbell and Bozorgnia (2003) $S_{VFS} = 0.25$, $S_{SR} = 0$ and $S_{FR} = 0$ as suggested by Table 5 of Campbell and Bozorgnia (2003). Stiff soil sites were assumed to have an average shear-wave velocity in the top $30\,\mathrm{m}$ of $420\,\mathrm{ms}^{-1}$ and hence be within category A ($360 < V_{s,30} \le 750\,\mathrm{ms}^{-1}$) of Ambraseys and Simpson (1996) and category B ($400 < V_{s,30} \le 800\,\mathrm{ms}^{-1}$) of Lussou *et al.* (2001) and for the equations of Campbell and Bozorgnia (2003) $S_{VFS} = 0$, $S_{SR} = 1$ and $S_{FR} = 0$ as suggested by Table 5 of Campbell and Bozorgnia (2003). Hard rock sites were assumed to have an average shear-wave velocity in the top $30\,\mathrm{m}$ of $800\,\mathrm{ms}^{-1}$ and hence be within category R ($V_{s,30} > 750\,\mathrm{ms}^{-1}$) of Ambraseys and Simpson (1996) and category A ($V_{s,30} > 800\,\mathrm{ms}^{-1}$) of Lussou *et al.* (2001) and for the equations of Campbell and Bozorgnia (2003) $S_{VFS} = 0$, $S_{SR} = 0$ and $S_{FR} = 1$ as suggested by Table 5 of Campbell and Bozorgnia (2003). A seismogenic distance of $10.4\,\mathrm{km}$ and a magnitude of $M_w = 6.5$ was used to compute the ratios for the equations of Campbell and Bozorgnia (2003); all the other ratios are independent of distance and magnitude.

a. Soft soil.

b. Stiff soil.

6. Comparison of the estimated median response spectra given by the equations presented here for strike-slip faulting (thick lines) and those presented by Ambraseys and Simpson (1996) (thin lines), which are independent of faulting mechanism.

    a. $M_w = 5.0$ ($M_s = 4.3$), $d_f = 10\,\mathrm{km}$.

    b. $M_w = 5.0$ ($M_s = 4.3$), $d_f = 100\,\mathrm{km}$.

    c. $M_w = 7.0$ ($M_s = 6.9$), $d_f = 10\,\mathrm{km}$.

    d. $M_w = 7.0$ ($M_s = 6.9$), $d_f = 100\,\mathrm{km}$.

7. Comparison of the estimated median response spectra given by the equations presented here (thick lines) and those presented by Campbell and Bozorgnia (2003) (thin lines) for strike-slip faulting.

    a. $M_w = 5.0$, $d_f = 10\,\mathrm{km}$ ($d_s = 10.4\,\mathrm{km}$).

    b. $M_w = 5.0$, $d_f = 100\,\mathrm{km}$ ($d_s = 100\,\mathrm{km}$).

    c. $M_w = 7.0$, $d_f = 10\,\mathrm{km}$ ($d_s = 10.4\,\mathrm{km}$).

    d. $M_w = 7.0$, $d_f = 100\,\mathrm{km}$ ($d_s = 100\,\mathrm{km}$).

8. Residuals against M_w and distance for PGA and SA at $1\,\mathrm{s}$. At the right-hand end of each residual plot there is a histogram using the residuals binned into 0.1 unit intervals.

    a. PGA.

    b. PGA.

    c. SA at $1\,\mathrm{s}$ natural period.

    d. SA at $1\,\mathrm{s}$ natural period.
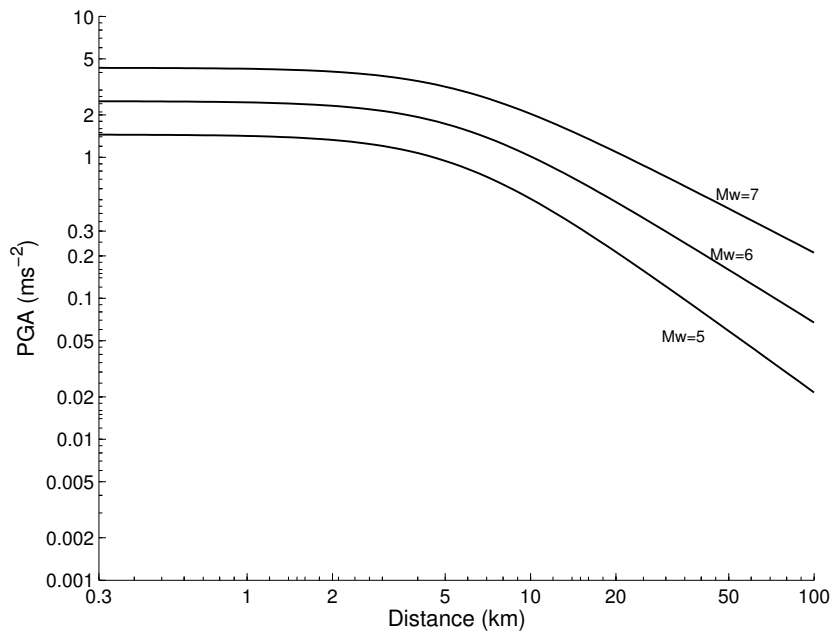
(a)
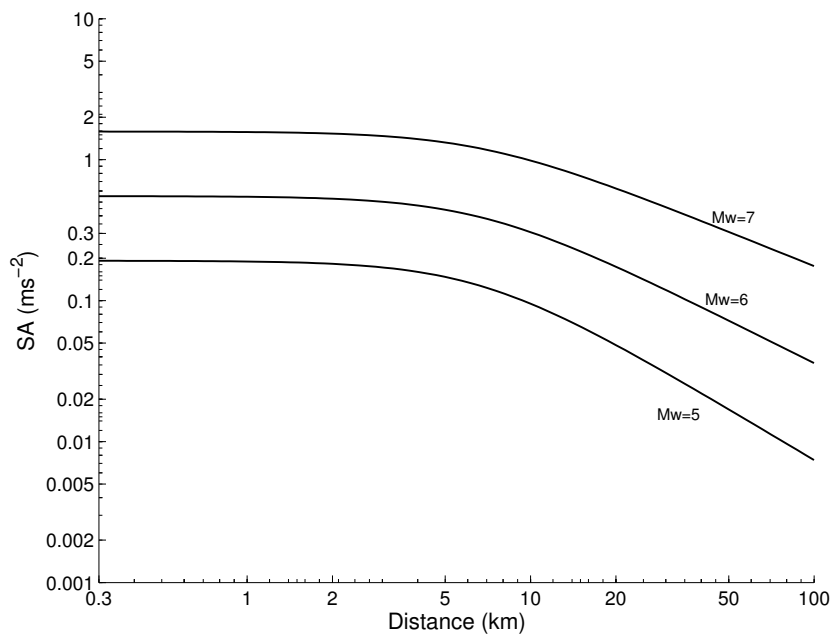
(b)

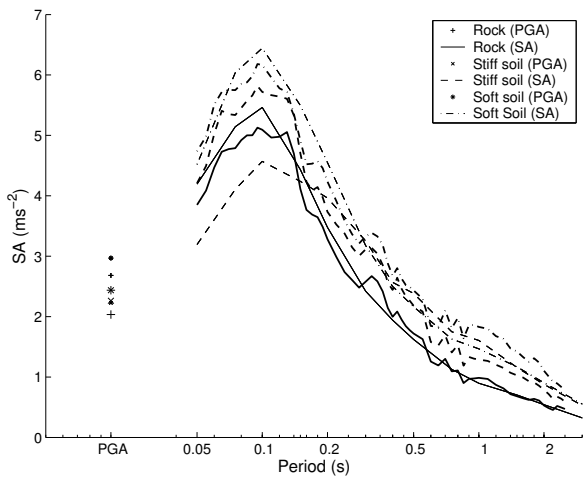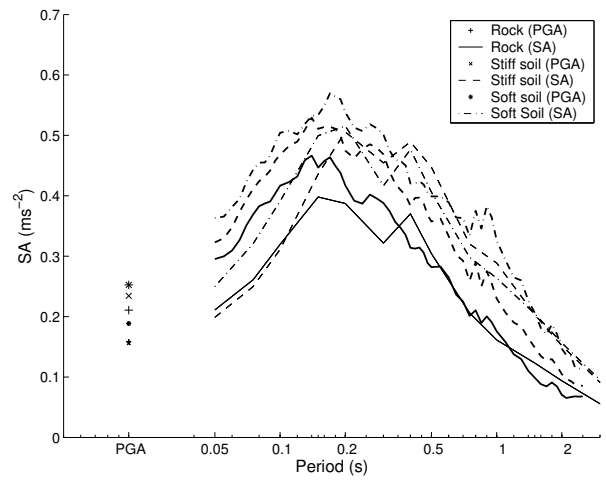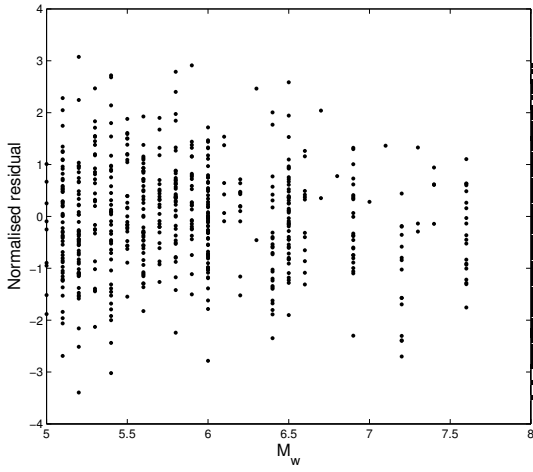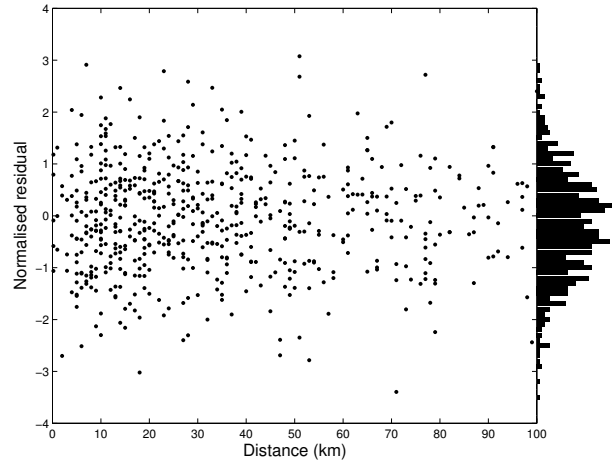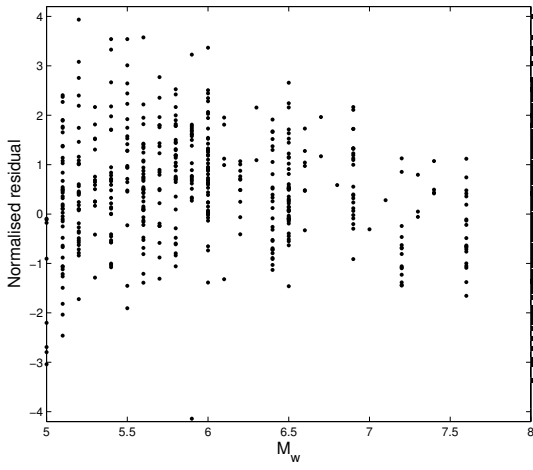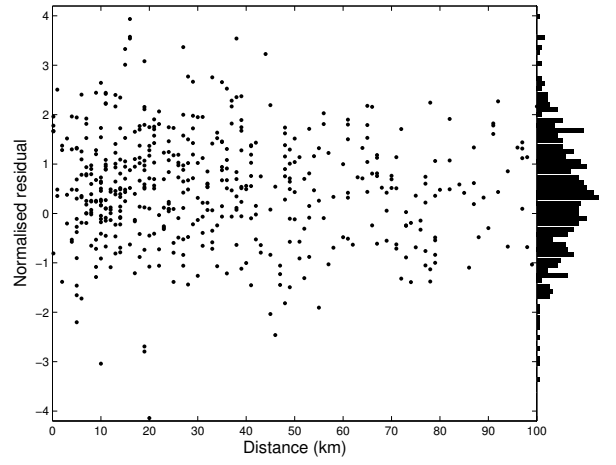Figure 1:
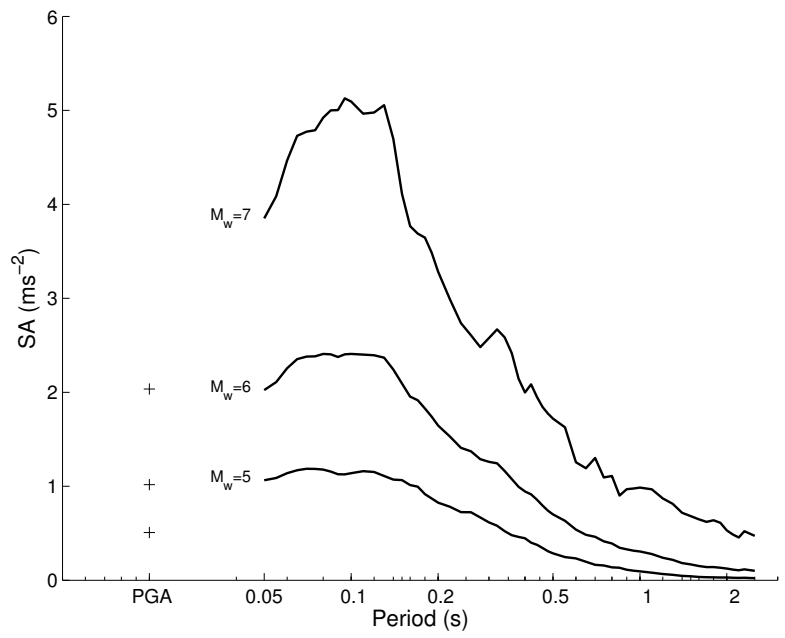
(a)
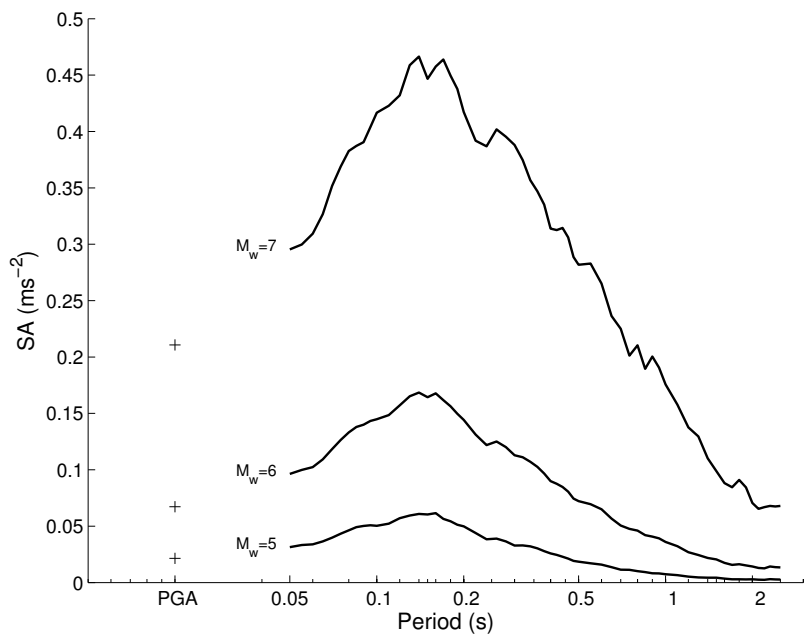
(b)

Figure 2:
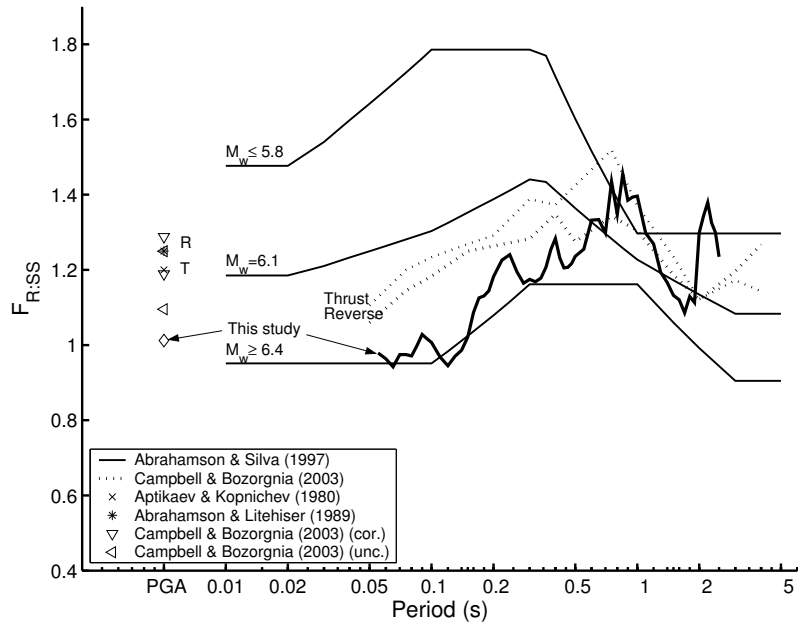
Figure 3:

Figure 4:

(a)

(b)

Figure 5:

Figure 6:

Figure 7:

(a)

(b)

(c)

(d)

Figure 8: